

Carbon nanotube-based nanoelectromechanical resonatoras mass biosensor

Ahmed M. Elseddawy, Adel H. Phillips, Ahmed S Bayoumi

Citation: Chin. Phys. B . 2020, 29(7): 078501 . **doi:** 10.1088/1674-1056/ab888f
Journal homepage: http://cpb.iphy.ac.cn; http://iopscience.iop.org/cpb

What follows is a list of articles you may be interested in

Design of a novel high holding voltage LVTSCR with embedded clamping diode

Ling Zhu(朱玲), Hai-Lian Liang(梁海莲), Xiao-Feng Gu(顾晓峰), Jie Xu(许杰)
Chin. Phys. B . 2020, 29(6): 068503 . **doi:** 10.1088/1674-1056/ab836e

Dark count in single-photon avalanche diodes: A novel statistical behavioral model

Wen-Juan Yu(喻文娟), Yu Zhang(张钰), Ming-Zhu Xu(许明珠), Xin-Miao Lu(逯鑫淼)
Chin. Phys. B . 2020, 29(4): 048503 . **doi:** 10.1088/1674-1056/ab7808

Numerical and analytical investigations for the SOI LDMOS with alternated high-*k* dielectric and step doped silicon pillars

Jia-Fei Yao(姚佳飞), Yu-Feng Guo(郭宇锋), Zhen-Yu Zhang(张振宇), Ke-Meng Yang(杨可萌), Mao-Lin Zhang(张茂林), Tian Xia(夏天)
Chin. Phys. B . 2020, 29(3): 038503 . **doi:** 10.1088/1674-1056/ab6960

Enhancement of radiation hardness of InP-based HEMT with double Si-doped plane

Ying-Hui Zhong(钟英辉), Bo Yang(杨博), Ming-Ming Chang(常明铭), Peng Ding(丁芃), Liu-Hong Ma(马刘红), Meng-Ke Li(李梦珂), Zhi-Yong Duan(段智勇), Jie Yang(杨洁), Zhi Jin(金智), Zhi-Chao Wei(魏志超)
Chin. Phys. B . 2020, 29(3): 038502 . **doi:** 10.1088/1674-1056/ab6962

High-throughput fabrication and semi-automated characterization of oxide thin film transistors

Yanbing Han(韩炎兵), Sage Bauers, Qun Zhang(张群), Andriy Zakutayev
Chin. Phys. B . 2020, 29(1): 018502 . **doi:** 10.1088/1674-1056/ab5d05

Carbon nanotube-based nanoelectromechanical resonator as mass biosensor

Ahmed M. Elseddawy[1,†], Adel H. Phillips[2,‡], and Ahmed S Bayoumi[3,§]

[1] *Faculty of Graduate Studies, University of Windsor, Windsor, Ontario, Canada*
[2] *Faculty of Engineering, Ain-Shams University, Cairo, Egypt*
[3] *Faculty of Engineering, Kafr-Elsheikh Unversity, Kafr-Elsheikh, Egypt*

(Received 1 February 2020; revised manuscript received 26 March 2020; accepted manuscript online 11 April 2020)

The use of single walled carbon nanotube-based nanoelectromechanical system (NEMS) resonator to sense the biomolecules' mass is investigated under the influence of an external ac-field. A single walled carbon nanotube (SWCNT) cantilever has been proposed and studied if the mass is attached at the tip or various intermediate positions. The shift of the resonant frequency and the quality factor have been investigated and show high sensitivity to the attached mass of biomolecule and its position. The proposed SWCNT-based NEMS resonator is a good candidate for sensing and tracing biomolecules' mass as concentration of acetone in human exhale, resulting in a painless, correct, and simple diabetics' diagnosis.

Keywords: single walled carbon nanotube, nanoelectromechanical system resonator, ac-field, biomolecule

PACS: 85.30.De, 72.80.Vp, 85.40.Qx **DOI:** 10.1088/1674-1056/ab888f

1. Introduction

Strides throughout nanotechnology resulted in novel tools which enhance fields of sensors and electronics. New engineered materials offer novel properties that enhance state-of-the-art components in cost, speed, power consumption, sensitivity, and density on chip.[1–7] single walled carbon nanotubes (SWCNTs) have attracted considerable attention for the last two decades.[8,9] Their unique mechanical, electrical, and optical properties have made them an attractive candidate for many applications.[10,12,13] Recently, mechanical properties of carbon nanotubes (CNTs) have inspired research.[14,15] Although applications focus primarily on bulk tensile strength, the low mass combined with the record Young's modulus about 1.2 TPa also results in extremely large increase in resonance frequency of SWCNT resonators.[16–20] CNTs are, also, expected to have major impact on several nanoelectromechanical system (NEMS) applications.[21–25]

NEMS technologies made it possible to detect physical quantities sensitively, such as spin,[21,26,27] molecular mass,[28–35] quantum states,[36] thermal fluctuation,[37] coupled resonance,[38,39] and biochemical reactions.[40,42] Also, NEMS technologies have allowed the rapid, reliable, and label-free detection of specific disease-related molecules, suggesting their potential in specific diseases early diagnosis such as cancer.[43–46] These impact values of NEMS offer motivations to proceed the investigation on the use of single walled carbon nanotube based NEMS resonator to sense trace acetone concentration in human exhale, resulting in a simple, reliable, and painless diabetics breath diagnosis.

The previous literature results[47] emphasized that the quality factor and resonant frequency shift of the proposed NEMS device are highly sensitive to the dimensions (length and diameter) of the SWCNT. The authors of Ref. [47] investigated the case when the biomolecule is only at the tip of the cantilever. Now, it is interesting to investigate the case when the biomolecule is at various intermediate positions along the SWCNT cantilever's length. There are four sections in this paper: the introduction, the theoretical model and its formalism, the numerical results for the proposed SWCNT based NEMS, and conclusion.

2. Theoretical model

The proposed model is a SWCNT cantilever acting as an NEMS resonator device which uses two leads in coupling with electronic transport. The influences of the induced ac-field and magnetic field are considered in the electron tunneling in the proposed device. Additional tunneling channels are induced when the carriers exchange energy with photons of energy $\hbar\omega$ from the induced ac-field of frequency ω, which represent photon-assisted tunneling.[48]

Figure 1 shows the SWCNT cantilever which is activated to vibrate in the y-direction. The shift of resonance frequency, $\Delta\upsilon$, and quality factor Q are given by[49]

$$|\Delta\upsilon| = \frac{\upsilon}{2}\cdot\frac{C_{\rm g}^2V_{\rm g}^2}{k_{\rm spring}C_{\rm CNT}}\left[\frac{2G}{C_{\rm CNT}\Gamma_{\rm withphotons}}-1\right], \quad (1)$$

†Corresponding author. E-mail: elsedda@uwindsor.ca
‡Corresponding author. E-mail: adel_phillips@eng.asu.edu.eg
§Corresponding author. E-mail:ahmed.bayoumi@eng.kfs.edu.eg

© 2020 Chinese Physical Society and IOP Publishing Ltd

$$\frac{1}{Q} = 2\pi\upsilon \frac{C_g^2 \cdot V_g^2}{k_{spring}} \left(\frac{2}{C_{CNT}\Gamma_{withphotons}} \right)^2 \cdot G, \quad (2)$$

where C_g is the coupling gate capacitance with SWCNT, C_{CNT} represents the carbon nanotube capacitance, the gate voltage is V_g, the probability of tunneling considering the photon-assisted tunneling (PAT) is Γ, and G represents the electronic conductance of SWCNT. The resonance frequency of the SWCNT cantilever in Eqs. (1) and (2) is represented as υ. This resonant frequency υ will take the following expression according to the following two cases:

(a) The first case in which the biomolecule is attached at the tip of the SWCNT cantilever (see Fig. 1(a)). So, the effective spring constant k_{spring} (see Eqs. (1) and (2) and the resonant frequency υ are given by[50,51]

$$k_{spring} = 3YI/L^3, \quad (3)$$

$$\upsilon = \frac{1}{2\pi}\sqrt{\frac{3\,(YI/L^3)}{0.24\rho AL + m_{bio\text{-}mol}}}, \quad (4)$$

where Y represents the Young's modulus of SWCNT, I represents its moment of inertia, the length of the SWCNT cantilever is L, ρ represents the density of SWCNT, A is its cross section area, and $m_{bio\text{-}mol}$ is the mass of the attached biomolecule.

(b) The second case in which the biomolecule is concentrated at any point along the SWCNT cantilever (see Fig. 1(b)). So, the effective spring constant k_{spring} (see Eqs. (1) and (2)) and the resonant frequency υ will take the following form:[50–52]

$$k_{spring} = 6YI/a^2\,(3L-a), \quad (5)$$

$$\upsilon = \frac{1}{2\pi}\sqrt{\frac{\left(\frac{6YI}{a^2\,(3L-a)}\right)}{0.24\rho AL + m_{bio\text{-}mol}}}, \quad (6)$$

where a represents the distance from the fixed end of the SWCNT cantilever at the moment when the biomolecule is positioned (see Fig. 1(b)).

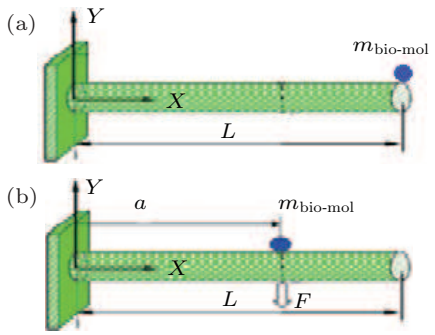


Fig. 1. Sketch of single walled carbon nanotube cantilever.

In Fig. 1(b), F is the weight of the attached biomolecule. Landauer–Buttiker formula[53,54] is used to calculate the device conductance G (Eqs. (1) and (2)

$$G = \frac{4e}{h}\sin\phi \int_{E_F}^{E_F + n\hbar\omega} dE \cdot \Gamma_{withPhoton}(E) \cdot \left(-\frac{\partial f_{FD}}{\partial E} \right), \quad (7)$$

where $-\partial f_{FD}/\partial E$ represents the first derivative of the Fermi–Dirac distribution function and is calculated as

$$\left(-\frac{\partial f_{FD}}{\partial E} \right) = (4k_B T)^{-1} \cdot \cosh^{-2}\left(\frac{E - E_F - n\hbar\omega}{2k_B T} \right).$$

Here, k_B is the Boltzmann constant, T is the absolute temperature, E is the tunneling carriers' energy, and E_F is the Fermi-energy.

The expression of $\Gamma_{withPhoton}$ has been derived by applying boundary conditions to the eigen-functions obtained through solving Dirac equation[55,56] as

$$\Gamma_{withPhoton} = \sum_{n=1}^{\infty} J_n^2\left(\frac{eV_{ac}}{\hbar\omega}\right) f_{FD}\left(E - \left(\frac{C_{CNT}}{C_g}\right)eV_g - n\hbar\omega - eV_{sd}\right) \times\Gamma_n(E + n\hbar\omega), \quad (8)$$

where J_n is the n^{th} order Bessel function of the first order appropriate to the n^{th} different side bands, V_{ac} represents the induced ac-field's peak value, the electron charge is e, the source–drain voltage is represented as V_{sd}, and f_{FD} represents the Fermi–Dirac distribution function. In Eq. (8), $\Gamma_n(E + n\hbar\omega)$ is calculated as[55,56]

$$\Gamma_n(E + n\hbar\omega) = \left| \frac{k_n}{k_n \cos\cos(k_n L) + \mathrm{i}\left(\frac{eV_g + eV_{sd} + \hbar eB/2m^*}{\hbar\omega}\right)\sin(k_n L)} \right|^2, \quad (9)$$

where the wave vector k_n is given by

$$k_n^2 = \left[\frac{V_b + eV_g + eV_{sd} + \hbar eB/m^*}{\hbar\omega} \right]^2 - q_n^2. \quad (10)$$

Here V_b represents the barrier height at the interface between the cantilever and leads, the applied magnetic field is represented by B, $\hbar$ represents the reduced Planck's constant, m^* represents the charge carrier's effective mass, and q_n can be calculated using the length, L, of the SWCNT cantilever

$$q_n = \frac{n'\pi}{L}, \quad n' = 1, 2, 3, \ldots \quad (11)$$

3. Results and discussion

The proposed biomolecule sensor based on the SWCNT system will be analyzed numerically for two cases; the biomolecule is positioned at the tip of the SWCNT cantilever in the first case, and in the second case, the biomolecule is at various intermediate positions. Acetone molecule is the aim of this investigation as the diabetic patients' exhale contains it.[51,57] And any biomolecule of the same mass rang would give consistent results.

The parameters in Eq. (7) for the conductance G[55,56] are $E_F = 0.125$ eV, $m^* = 0.054 m_e$ (where m_e represents the free electron mass), $C_g = 0.4$ nF, and $C_{CNT} = 0.25$ nF. This investigation focuses on constant diameter and so that constant Young's modulus and density, and the effect of the SWCN diameter variation is not considered.

Figure 2 illustrates the behavior of conductance G with photon energy, E, of the induced ac-field at various magnitudes of the applied magnetic field, B. This figure shows an oscillatory behavior of conductance with different peak heights, small side resonant peaks surrounding the main resonant peaks. The cause of the small side-peaks might be the PAT procedure such as the photon absorption and emission.[48] Ac-field induces shifts in the energy levels, causing resonant peaks at positions of photonic sidebands characterized by $n = 0, \pm 1, \pm 2, \ldots$ The observed peak height (see Fig. 2) is determined by a Bessel function (see Eq. (8)).[48,58] It is also noticed that with the increase of the photon energy, the peak height increases. This profile of the conductance with the photon energy could be due to the photon induced sideband resonances.[55,56,58] As the induced photons' energy increases, the interaction between them and transport carriers strongly increases, and this interaction affects the sidebands and tunneling rates.[48,55,58]

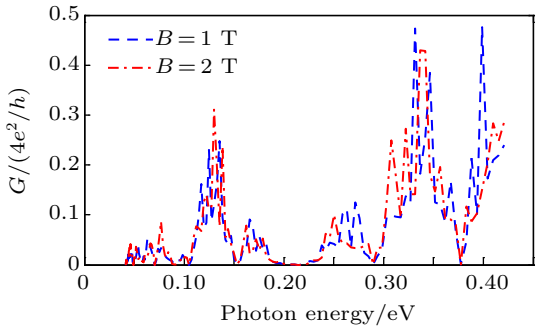


Fig. 2. The behavior of conductance, G, with photon energy at various magnitudes of the applied magnetic field.

(i) Results for the first case when the biomolecule is positioned at the tip of the SWCNT cantilever: the Young's modulus of CNT is equal to 1.0×10^{15} ng/nm·s^2 and its density $\rho = 1.4 \times 10^{-12}$ ng/nm^3.[47,51,56,57]

Figure 3(a) illustrates the behavior of resonant frequency shift $\Delta\upsilon$ versus the attached biomolecule mass $m_{\text{bio-mol}}$ at different photon energies. As shown in the figure, the resonant frequency shift decreases as the mass of the attached biomolecule increases. Also, we notice from this figure that the resonant frequency shift $\Delta\upsilon$ is very small, approximately 10^{-6} Hz. This small value of $\Delta\upsilon$ could be obtained by measuring the conductance, G, of the carbon nanotube device. It is known that the conductance of nanostructured devices could be measured with a high precision. It is well known that the SWCNT has been proposed as THz (infrared region) oscillators for novel applications as NEMS.[59,60] These ranges of frequencies are consistent with the induced photon energy of the ac-field (infrared region). This coupling between the mechanical vibration of the SWCNT and the applied photon energy affects prominently on the mass sensitivity.

Figure 3(b) illustrates the behavior of the quality factor inverse, $(1/Q)$, versus the mass of the attached biomolecule, $m_{\text{bio-mol}}$, at different photon energies. As shown in this figure, the inverse quality factor decreases as the mass of the attached biomolecule increases. Also the inverse quality factor increases as the photon energy of the induced ac-field increases. The higher quality factor (Q-factor) means higher sensitivity and more reliable performance of the present SWCNT based NEMS.[61] This sensitivity of Q-factor increases as the photon energy of the induced ac-field increases.

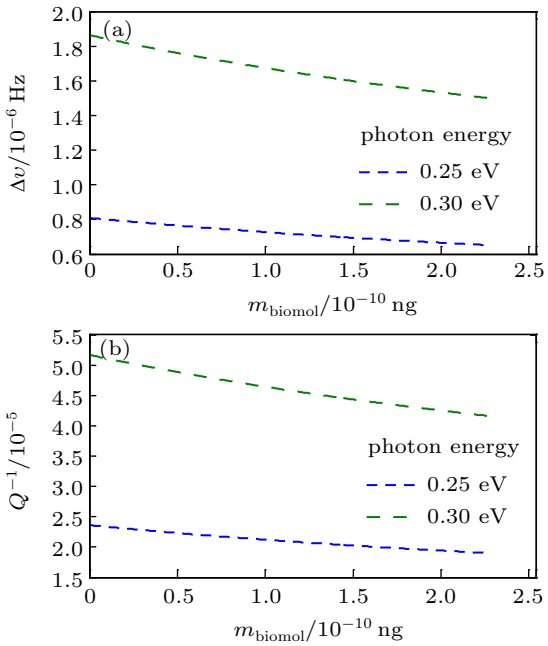


Fig. 3. The behavior of (a) resonant frequency shift $\Delta\upsilon$ and (b) the inverse of the quality factor, $(1/Q)$, versus the mass of the biomolecule at various photon energies.

(ii) Results for the second case when the biomolecule is at various intermediate positions on the SWCNT cantilever.

Figure 4(a) illustrates the behavior of resonant frequency shift $\Delta\upsilon$ versus the attached biomolecule mass $m_{\text{bio-mol}}$ for the biomolecule at different positions a. We notice from this figure that $\Delta\upsilon$ is higher when $a = 4$ nm, that is, at a position of about 33% of the SWCNT cantilever length, ($L = 12$ nm), compared to the other positions $a = 6$ nm and $a = 8$ nm.[32,52] For the three positions, $\Delta\upsilon$ decreases as $m_{\text{bio-mol}}$ increases.

Figure 4(b) illustrates the behavior of the quality factor inverse $(1/Q)$ versus the biomolecule mass for the biomolecule at different positions a. As shown in the figure, for all three intermediate positions, the inverse quality factor $(1/Q)$ decreases as the mass $m_{\text{bio-mol}}$ increases. Also, $(1/Q)$ is the highest for the case when $a = 4$ nm, which is 33% of the length of SWCNT $L = 12$ nm.

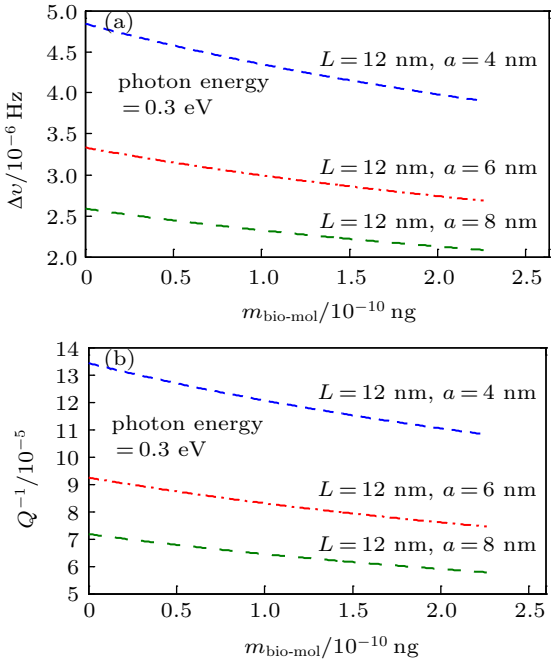


Fig. 4. The behavior of (a) resonant frequency shift $\Delta\upsilon$ and (b) the variation of $(1/Q)$ with $m_{\text{bio-mol}}$ at different a.

In order to confirm the effect of the photon energy of the induced ac-field on both quality factor Q and resonant frequency shift $\Delta\upsilon$, the calculations are performed for the case when $a = 7$ nm, that is, 58% of the total length $L = 12$ nm. The results are shown in Figs. 5(a) and 5(b). As shown, $\Delta\upsilon$ and $(1/Q)$ increase as the photon energy increases. This effect of photon energy shows that the interaction between photon and mechanical vibration of the SWCNT plays an important role in the mass sensitivity. The results are found to be consistent with those in the literature.[50,51,62–65]

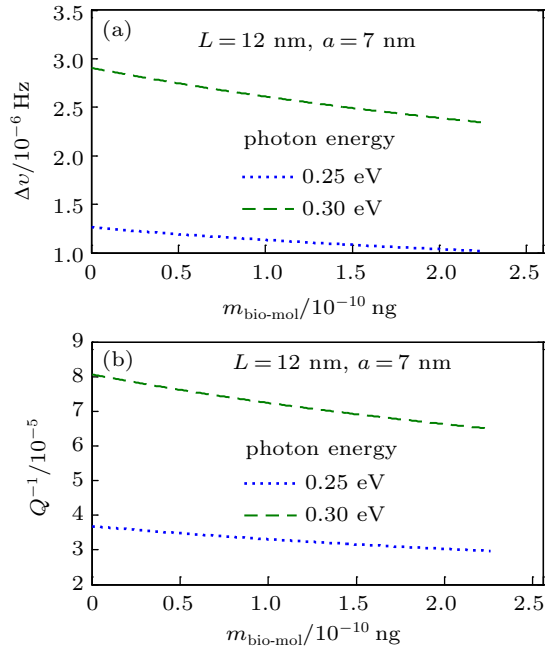


Fig. 5. The behavior of (a) $\Delta\upsilon$ and (b) the variation of $(1/Q)$ with $m_{\text{bio-mol}}$ at different photon energy.

4. Conclusion

SWCNT based sensor is investigated under effect of induced ac-field's photons in the infrared region. The case of mass sensing studied is the biomolecule acetone which exists in the diabetic patients' exhale. Results illustrate that the quality factor and change in resonant frequency are delicate to the attached biomolecule mass and its position. Also, the induced ac-field affects on both quality factor and change in resonant frequency. So, the SWCNT based nanoelectromechanical resonator could be used to sense acetone molecules and consequently for diabetes diagnosis.

References

[1] Cao Y Q, Huang H L, Sun Z H, Li F Y, Bai H L, Zhang H, Sun N and Yung C 2019 *Acta Phys. Sin* **68** 158502 (in Chinese)
[2] Ye S J, Li C Z, Zhang J H, Tan J J and Luo Y 2019 *Acta Phys. Sin.* **68** 013101 (in Chinese)
[3] Xiaolong C, Dong Z, Liang C, Fangfang R, Hong Z, Rong Z, Youdou Z and Hai L 2019 *Chin. Phys. B* **28** 098503
[4] Fei H, Ruibo C, Feibo D, Jizhi L, Zhiwei L and Juin J L 2019 *Chin. Phys. B* **28** 088501
[5] Slimane L, Mohamed F and Abderrahmane K 2019 *Chin. Phys. B* **28** 088801
[6] Shu X S, Ming M C, Meng K L, Liu H M, Ying H Z, Yu X L, Peng D, Zhi J and Zhi C W 2019 *Chin. Phys. B* **28** 078501
[7] Zheng X W, Feng Z, Zhan W S, Jun C, Ya W H, Guo G Y, Xing F L, Wan S Z, Lei W, Guo S S, Yi P Z 2019 *Chin. Phys. B* **28** 068504
[8] Iijima S 1991 *Nature* **354** 56
[9] Iijima S and Ichihashi T 1993 *Nature* **363** 603
[10] Treacy M M J, Ebbesen T W, and Gibson J M 1996 *Nature* **381** 678
[11] Tans S J, Vershueren A R M and Dekker C 1998 *Nature* **393** 49
[12] De-Heer W A, Chatelain A and Ugarte D 1995 *Science* **270** 1179
[13] Kong J, Franklin N R, Zhan C W, Chapline M G, Peng S, Cho K J and Dai H J 2000 *Science* **287** 622
[14] Lu J P 1997 *Phys. Rev. Lett.* **79** 1297
[15] Yu M F, Files B S, Repalli S A and Ruoff R S 2000 *Phys. Rev. Lett.* **84** 5552
[16] Sazonova V, Yaish Y, Ustunel H, Roundy D, Arias T A and McEuen P L 2004 *Nature* **431** 284
[17] Witkamp B, Poot M and Zant H V 2006 *Nano Lett.* **6** 2904
[18] Reulet B, Kasumov V Y, Kociak M, Deblock R, Khodos I I, Gorbatov Y B Volkov V T, Journet C and Bouchiat H 2000 *Phys. Rev. Lett.* **85** 2829
[19] Wang K and Wang B 2016 *J. Vib. Control* **22** 1405
[20] Natsuki T 2017 *Electronics* **6** 56
[21] Schmid S, Villanueva L G and Roukes M L 2016 *Fundamentals of Nanomechanical Resonators* (Berlin: Springer International Publishing)
[22] Sinha N, Ma J and Yeow J T W 2006 *J. Nanosci. Nanotechno.* **6** 573
[23] Huttel A K, Meerwaldt H B, Steele G A, Poot M, Witkamp B, Kouwenhoven L P and van der Zant H S J 2010 *Phys. Status Solidi B* **247** 2974
[24] Schmid D R, Stiller P L, Strunk Ch and Huttel A K 2012 *New J. Phys.* **14** 083024
[25] Soltani P, Pashaei O, Taherian M M and Farshidianfar A 2012 *Adv. Mater. Res.* **403–408** 1163
[26] Rugar D, Budakian R, Mamin H J and Chui B W 2004 *Nature* **430** 329
[27] Budakian R, Mamin H J and Rugar D 2006 *App. Phys. Lett.* **89** 113113
[28] Yang Y T, Callergari C, Feng X L, Ekinci K L and Roukes M L 2006 *Nano Lett.* **6** 583
[29] Li M, Tang H X and Roukes M L 2007 *Nat. Nanotechnol.* **2** 114
[30] Jensen K, Kin K and Zettl A 2008 *Nat. Nanotechnol.* **3** 533
[31] Naik A K, Hanay M S, Hiebert W K, Feng X L and Roukes M L 2009 *Nat. Nanotechnol.* **4** 445
[32] Joshi A Y, Harsha S P and Sharma S C 2010 *Physica E* **42** 2115
[33] Chaste J, Eichler A, Moser J, Ceballos G, Rurali R and Bachtold A 2012 *Nat. Nanotechnol.* **7** 301
[34] Arash B and Wang Q 2013 *Sci. Rep.* **3** 1

[35] Sireesha M, Babu V J, Kiran A S K and Ramakrishna S 2018 *Nanocomposites* **4** 36
[36] Cheland A N and Geller M R 2004 *Phys. Rev. Lett.* **93** 070501
[37] Tamayo J, Calleja M, Ramos D and Mertens J 2007 *Phys. Rev. B* **76** 180201
[38] Spletzer M, Raman A, Wu A Q, Xu X F and Reifenberger R 2006 *Appl. Phys. Lett.* **88** 254102
[39] Shim S B, Imboden M and Mohanty P 2007 *Science* **316** 95
[40] Kwon T, Eom K, Park J, Yoon D S, Lee H L and Kim T S 2008 *Appl. Phys. Lett.* **93** 173901
[41] Eoma K, Park H S, Yoonc D S and Kwonc T 2011 *Phys. Rep.* **503** 115
[42] Zhou Y, Fang Y and Ramasamy R P 2019 *Sensors* **19** 392
[43] Goeders K M, Colton J S and Bottomley L A *Chem. Rev.* **108** 522
[44] Natsuki T 2017 *Electronics* **6** 56
[45] Choi H K, Lee J, Park Mi K and Oh J H 2017 *J. Food Qual.* 5239487
[46] Same S and Samee G 2018 *CJMB Sciences* **5** 1
[47] Elseddawy A M, Zain W A and Phillips A H 2012 *J. Am. Sci.* **8** 566
[48] Platero G and Aguado R 2004 *Phys. Rep.* **395** 1
[49] Lassagne B, Tarakanov Y, Kinaret J, Garcia-Sanchez D and Bachtold A 2009 *Science* **325** 1107
[50] Wu D H, Chien W T, Chen C S and Chen H H 2006 *Sensor Actuat A Phys.* **126** 117
[51] Chowdhurg R, Adhikari S, and Mitchell J 2009 *Physica E* **42** 104
[52] Joshi A Y, Sharma S C and Harsha S P 2008 *Int. J. Electrospun Nanofibers Applications* **2** 161
[53] Ferry D K and Goodnik S M 1997 *Transport in Nanostructures* (New York: Cambridge University Press)
[54] Bosnick K, Gabor N and Paul M 2006 *App. Phys. Lett.* **89** 163121
[55] Mina A N, Awadallah A A, Phillips A H and Ahmed R R 2010 *Prog. Phys.* **4** 61
[56] Awadallah A A, Phillips A H, Mina A N and Ahmed R R 2011 *Int. J. Nanosci.* **10** 419
[57] Deng C, Zhang J, Yu X, Zhang W and Zhang X 2004 *J Chromatogr B Analyt Technol Biomed Life Sci.* **810** 269
[58] Meyer C, Elzerman J M and Kouwenhoven L P 2007 *Nano Lett.* **7** 295
[59] Stampler C, Jungen A, Linderman R, Obergfell D, Roth S and Hierold C 2006 *Nano Lett.* **6** 1449
[60] Singh G, Rice P and Mahajan R L 2007 *Nanotechnol.* **18** 475501
[61] Li C and Chou T W 2003 *Phys. Rev. B.* **68** 073405
[62] Scarpa F and Adhikari S 2008 *J. Non-Cryst Solids* **354** 4151
[63] Ekinci K and Roukes M 2005 *Rev. Sci. Instrum.* **76** 061101
[64] Aydogdu M and Filiz S 2011 *Physica E* **43** 1229
[65] Li J J and Zhu K D 2013 *Phys. Rep.* **525** 223